Advanced Composite Materials
Publication details, including instructions for authors and subscription information:
http://www.tandfonline.com/loi/tacm20

Characterization of fracture process during ring burst test of FW-FRP composites with damage

Akihiro Horide [a], Shuichi Wakayama [b] & Masanori Kawahara [c]

[a] Department of Mechanical Engineering, Tokyo Metropolitan University, 1-1 Minami-Ohsawa, Hachioji-shi, Tokyo 192-0397, Japan

[b] Department of Mechanical Engineering, Tokyo Metropolitan University, 1-1 Minami-Ohsawa, Hachioji-shi, Tokyo 192-0397, Japan

[c] Department of Mechanical Engineering, Tokyo Metropolitan University, 1-1 Minami-Ohsawa, Hachioji-shi, Tokyo 192-0397, Japan

Version of record first published: 02 Apr 2012.

To cite this article: Akihiro Horide , Shuichi Wakayama & Masanori Kawahara (1999): Characterization of fracture process during ring burst test of FW-FRP composites with damage, Advanced Composite Materials, 8:2, 139-151

To link to this article: http://dx.doi.org/10.1163/156855199X00155

howsoever caused arising directly or indirectly in connection with or arising out of the use of this material.

Adv. Composite Mater., Vol. 8, No. 2, pp. 139–151 (1999)

Characterization of fracture process during ring burst test of FW–FRP composites with damage

AKIHIRO HORIDE*, SHUICHI WAKAYAMA and MASANORI KAWAHARA

Department of Mechanical Engineering, Tokyo Metropolitan University, 1-1 Minami-Ohsawa, Hachioji-shi, Tokyo 192-0397, Japan

Received 20 June 1998; accepted 17 August 1998

Abstract—The strength of two- and three-ply FRP composite with artificial damage under internal pressure was evaluated using the ring burst test developed by the authors [1, 2]. Ring specimens were fabricated by a filament winding (FW) machine. In this study, the simulated damage of the scratch and the combination of scratch and pre-existing interlaminar delamination, i.e. teflon sheet inserted between the outermost and the inner FRP layers, were introduced artificially into the FW–FRP specimen. The fracture behavior during the tests of damaged FRP was characterized by observation using an 8-mm video camera and a high magnification video scope, strain measurements and AE analysis. It was confirmed that AE analysis is exellent for monitoring the propagation of delamination in an FRP pressure vessel with damage. The pressure of a notched specimen showed the maximum when the delamination propagated to the half region of the specimen. The maximum pressure was larger than the predicted pressure based on the premise that the notched outermost ply could not sustain the load. As the teflon sheet was longer, the maximum pressure was gradually decreased due to the decrease in initial ligament. On the other hand, as the teflon sheet was longer, the burst pressure of specimen with a scratch in the outermost ply was enhanced due to the smooth propagation of interlaminar delamination. Consequently, it was demonstrated by the observation of the fracture behavior and the fracture surface that the burst pressure was decreased due to the expansion of damage into the inner ply.

Keywords: FRP composite; filament winding; interlaminar fracture behavior; delamination; ring burst test; AE analysis.

1. INTRODUCTION

FW–FRP pressure vessels have been developed and applied to the air containers used for breathing apparatus [3] and the fuel gas containers of compressed natural gas (CNG) vehicles [4] because of their high specific strength. It is generally known that interlaminar delamination, matrix cracking and fiber breakage are initiated when the FRP is subjected to an impact load [5]. Moreover, if the impact load

*To whom correspondence should be addressed. E-mail: horide@mech.metro-u.ac.jp

is applied at the sharp edge, a severe flaw such as a scratch will be introduced on the surface of the FRP layer in addition to this damage. Therefore, it is an important subject for the designer dealing with composite materials to characterize the fracture behavior of a damaged composite and to estimate the residual strength.

In order to characterize the fracture behavior of damaged FRP and evaluate the fracture toughness, many studies on each fracture mode have been carried out [6–9]. However, since the stress states of those tests are quite different from the internal pressure test, the new testing technique simulating internal pressure, the ring burst test, has been developed and applied to the evaluation of the effects of fiber waviness on the burst strength [10]. It is important that the interlaminar fracture behavior in an FRP composite can be observed during the test by a high magnification video scope.

In this study, for the investigation of the fracture behavior during the ring burst test of FRP composites with damage, a notch and a teflon sheet were introduced into the specimens, which simulated a scratch and a pre-existing interlaminar delamination, respectively. Moreover, this combination was introduced as an impact damage at the sharp edge. The fracture behavior was characterized by observations using an 8-mm video camera and a high magnification video scope, strain measurements, and AE analysis. Consequently, the effects of damage on the fracture behavior and the strength of FW–FRP composite were evaluated.

2. EXPERIMENTAL PROCEDURE

2.1. Preparation of damaged ring specimens

The two- or three-ply FRP ring specimens were made from E-glass fiber (diameter: 16 μm, roving tensile strength: 1.9 GPa) and epoxy resin. The fiber roving with the epoxy resin was wound along the hoop direction on an aluminum tube (outer diameter: 100 mm, thickness: 3 mm) by a filament winding machine, where the tension in the fiber roving was controlled as constant. After curing in an oven, the FRP wound on aluminum tubes were cut into ring specimens of 10 mm in width.

Table 1 summarizes the specimen types and the combinations of damage. In this study, the following two types of simulated damage were introduced into the FW–FRP specimens. In order to simulate the scratch, a notch was introduced by a 0.7-mm width cutting wheel mechanically. The notch orientation was perpendicular to the fiber direction and the notch depth in each specimen was approximately 0.4 mm, i.e. the thickness of the outermost ply. The combination of notch and pre-existing interlaminar delamination was introduced into the FW–FRP specimens as impact damage at the sharp edge. The pre-existing interlaminar delamination was introduced by inserting a teflon sheet (thickness: 0.05 mm) between the outermost and the inner FRP layers during fabrication. In the specimens with combined damage, the notch was introduced at the center of both pre-existing delamination tips and the notch root was located on the surface of the delamination. In order

to investigate the effect of pre-existing interlaminar delamination length, i.e. initial ligament length, on the strength in FRP composite with a scratch, several lengths of teflon sheet were used as shown in Table 1.

2.2. Ring burst test

In this study, the ring burst tests developed by the authors were applied to the evaluation of the strength and the observation of fracture behavior in FW–FRP pressure vessels subjected to internal pressure. A schematic drawing of the ring burst test equipment is shown in Fig. 1. The internal pressure was generated by means of inserting a tapered rod into twelve piece steel segments. The specimen was then pressurized through an urethane rubber ring located between the specimen and the twelve piece segments. It was confirmed by the finite element analysis and the strain measurements that the stress distribution could be considered as uniform [2]. Since the internal pressure applied to the specimen could not be measured directly in the ring burst test, preparatory experiments were carried out

Table 1.
Specimen types and combinations of damage

Specimen type	Number of ply	Combination of damage	
		Notch	Length of teflon [mm]
ND-2	2	×	—
N-2		○	—
N/T10-2		○	10
N/T20-2		○	20
ND-3	3	×	—
N-3		○	—
N/T10-3		○	10
N/T20-3		○	20
N/T40-3		○	40
N/T80-3		○	80
N/T150-3		○	150
N/T300-3		○	300

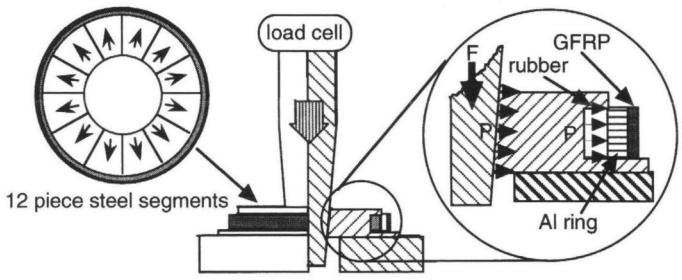

Figure 1. Schematic drawing of ring burst test equipment.

and a linear relationship between the corresponding internal pressure and the axial load of the rod was obtained [10]. The ring burst test has the following advantages. (1) Conditions of internal pressure can be simulated by the twelve divided segments and a urethane rubber ring. (2) The *in situ* observation of inter- and/or intralaminar fracture behavior is practicable. (3) Since the simple strength evaluation using the ring burst test can be carried out at low cost, a number of similar tests can be repeated easily. Recently, the authors have found, by a number of ring burst tests, that the burst pressure of multiply FW–FRP composite was strengthened by control of the tension in the fiber roving [10].

2.3. *Characterization of fracture behavior*

In order to characterize the fracture behavior of damaged FW–FRP composite, observation using an 8-mm video camera and a high magnification video scope, strain measurements and AE analysis were carried out. The positions of strain gages and AE sensors are shown in Fig. 2. Strain gages attached on the specimen surface were used to monitor the macroscopic delamination propagation at each gage position. Especially, the strain gages at the teflon tips were used to detect the onset of propagation from the tips of pre-existing interlaminar delamination. The characterization system diagram of delamination propagation is shown in Fig. 3, schematically. The

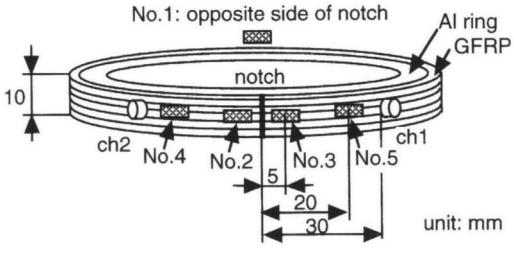

Figure 2. Schematic drawing of configurations of strain gages and AE sensors on notched specimen.

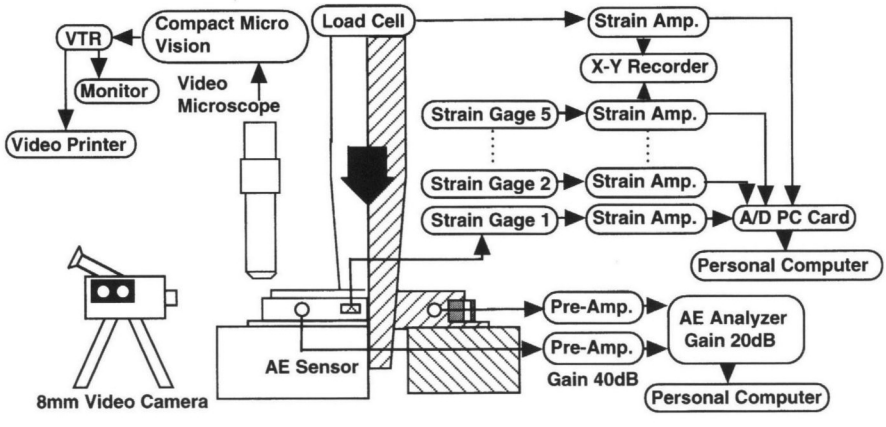

Figure 3. Characterization system of delamination propagation.

macroscopic propagation behavior of delamination was observed by an 8-mm video system. A high magnification video scope system was also used to observe the microscopic fracture process in the vicinity of the notch root and the tip of pre-existing interlaminar delamination.

In order to analyze the fracture behavior and to develop the technique for the inspection of pre-existing interlaminar delamination in FW–FRP pressure vessel, AE measurements were also carried out. The total gain was 60 dB (20 dB at the main amplifier and 40 dB at the pre-amplifier), and the threshold level was 45 dB (i.e. 177 μV at the input terminal of the pre-amplifier). Two channel sensors with resonant frequency of 500 kHz were attached on the specimen surface and the distance between the sensors was 60 mm. The AE signals were measured by an AE system, sent to a personal computer and analyzed in detail.

3. EXPERIMENTAL RESULTS

3.1. Fracture behavior of specimen during ring burst test

Typical internal pressure and outermost ply hoop strain–time curves of type N-3, a notched three-ply specimen, are shown in Fig. 4a. In the figure, points A, B, C, and D indicate the strain decreasing points of strain gage No. 2 (and 3), No. 5, No. 1, and No. 4, respectively. Since the corresponding expansion of matrix crazing was observed by an 8-mm camera, it was understood that the decrease in each strain indicated the propagation of delamination tip at each strain gage position. The detailed fracture behavior is summarized below.

(1) At 170 s, the initiation and the onset of propagation of delamination at the notch root was observed by a high magnification video scope.

(2) At point A, it was observed that the tip of delamination reached at strain gage No. 2 and 3 by an 8-mm video camera.

(3) At point B, the tip of delamination reached at strain gage No. 4.

(4) At point C, the pressure and the strain of No. 1 gage attached on opposite sides of the notch were decreased at the maximum pressure, P_{max}, when the delamination propagated to half region of specimen.

(5) At point D, the delamination rapidly propagated and then all of the plies burst at the burst pressure, P_{burst}.

On the other hand, for type N/T10-3 specimen with combined damage, the strain behaviors indicating the propagation of delamination are shown in Fig. 4b. In this specimen, the tips of pre-existing interlaminar delamination were located at the strain gages No. 2 and 3. The strain of No. 2 and 3 gages reached to the maximum ($\varepsilon_{max.2}$ and $\varepsilon_{max.3}$, respectively) and decreased at 100 s. At the same time, the onset of the propagation of delamination from the tip of pre-existing interlaminar delamination along the fiber direction and the expansion of matrix crazing were observed. Although the maximum strains, $\varepsilon_{max,2}$ and $\varepsilon_{max.3}$, are lower, other strain behaviors were similar to those of type N-3 specimen.

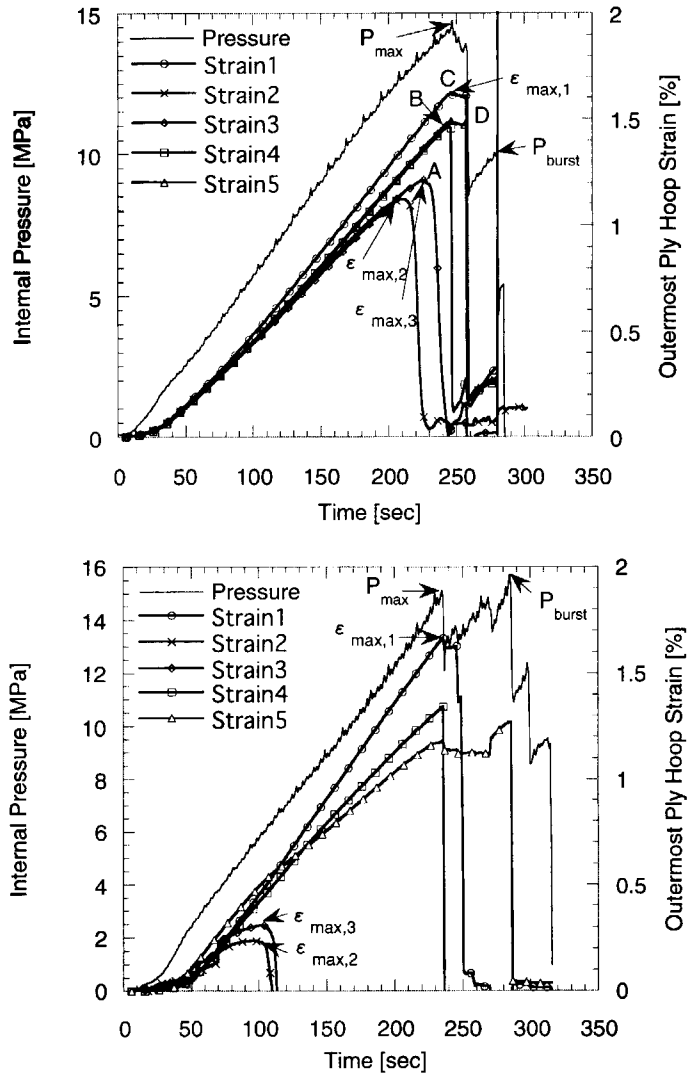

Figure 4. Results of strain measurement expressing delamination propagation. (a) Type N-3 specimen (3-ply, notch). (b) Type N/T10-3 specimen (3-ply, notch and teflon sheet 10 mm in length).

3.2. AE analysis

The AE source location was determined by measuring the differences in the wave arrival time between two channel AE sensors. In this study, the wave velocity in FRP composite material was calibrated by preparatory experiments using simulated AE sources. In unnotched specimens, AE locations were distributed widely through the specimen during ring burst tests. On the other hand, the AE locations of type N/T10-2, notched two-ply specimen with teflon sheet in 10 mm length, are shown in Fig. 5 and the results of strain measurements of the identical specimen

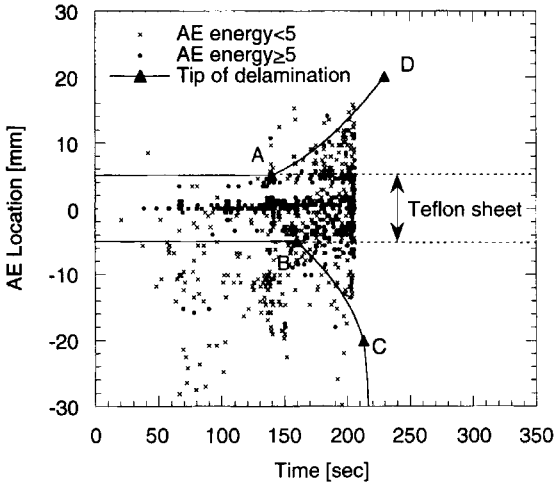

Figure 5. AE locations and delamination tip determined from strain measurement in type N/T10-2.

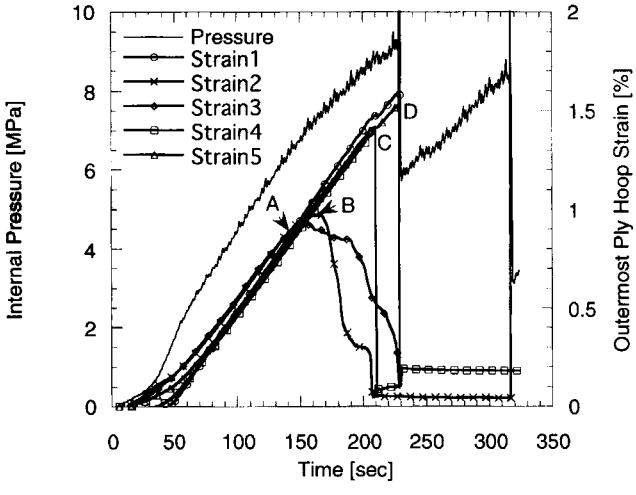

Figure 6. Result of strain measurements expressing delamination propagation of specimen in Fig. 5.

are shown in Fig. 6. In the figures, points A, B, C, and D indicate that tips of delamination reach the strain gages No. 3, 2, 4, and 5, respectively. It can be seen from Fig. 5 that AE locations with higher energy concentrate at the notch root until 140 s, and then they are widened from not only the notch root but also the teflon tips as the interlaminar delamination propagates. Therefore, it is considered that the expansion of delamination and the debonding within the area of teflon sheet occur simultaneously by the circumference deformation of the notched outermost ply. Comparing the results of an AE analysis and strain measurements, it is understood that the AE locations with high energy show good agreement with the delamination propagations. It can be concluded by

consideration of the mechanical features of fracture behavior in damaged FRP that AE signals with higher energy are related to the interlaminar friction at delamination.

From these results, it is understood that the AE technique is more powerful than strain measurements for the inspection of pre-existing interlaminar delamination and the monitoring of interlaminar delamination propagation in an FW–FRP pressure vessel with damage, because the detectable area of AE analysis is larger than the observable area of strain measurements.

3.3. Strength of damaged ring specimen

The maximum, P_{max}, and burst pressure, P_{burst}, of two- and three-ply FRP ring specimens are shown in Fig. 7a and b, respectively. ROM is the ideal fracture pressure calculated from the rule of mixture by the following procedure.

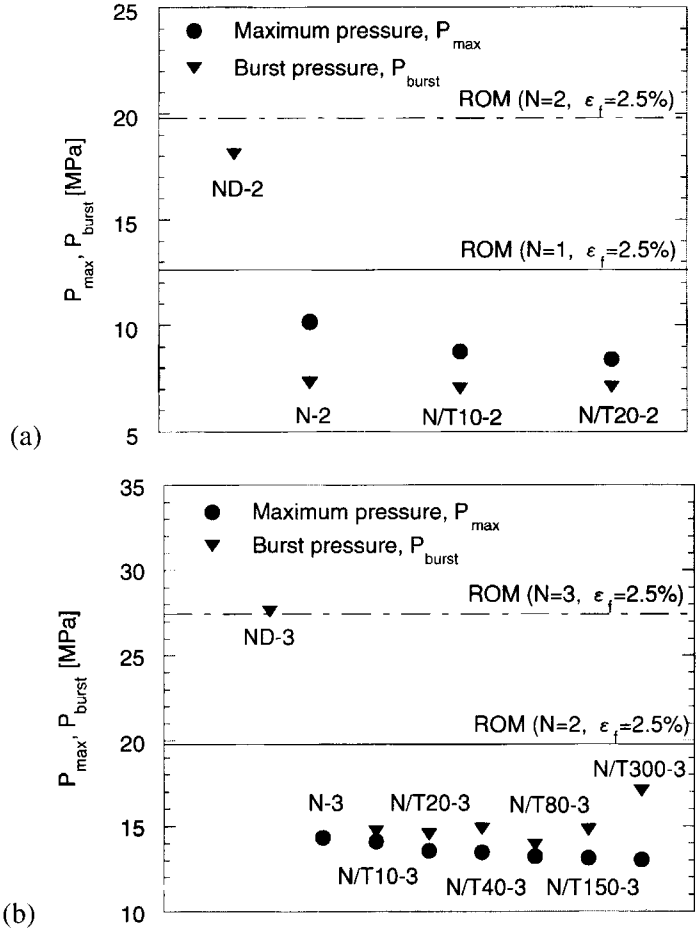

Figure 7. Strength of ring specimens with damage: (a) 2-ply specimens; (b) 3-ply specimens.

Assuming that the aluminum ring and each FRP layer are thin-walled cylinders and the fiber stress is larger enough than the matrix stress, the pressure of aluminum ring, $P_{f,Al}$, and each FRP layer, $P_{f,FRP}$, at the fracture of FRP layers are given by

$$P_{f,Al} = \sigma_{f,Al}\frac{t_{Al}}{r_{Al}}, \tag{1}$$

$$P_{f,FRP} = \sigma_{f,FRP}\frac{t_{FRP}}{r_{FRP}} = \sigma_{f,fiber}\frac{t_{fiber}}{r_{FRP}}, \tag{2}$$

where σ_f is the hoop stress at the fracture of FRP layers; t is the thickness and r is the inner radius. The subscripts Al, fiber and FRP denote the aluminum ring, fiber roving, and FRP ply, respectively. For simplification, r_{FRP} and t_{FRP} were considered as constant for each FRP layer. Since the linear relationship between the hoop stress and strain holds until final fracture, the fracture strength of fiber roving, $\sigma_{f,fiber}$, can be expressed as $E_{fiber} \cdot \varepsilon_f$, using the Young's modulus of fiber, E_{fiber}, and the fracture hoop strain of FRP ply, ε_f. Summing the $P_{f,Al}$ and $P_{f,FRP}$, the ideal fracture pressure in an N-ply specimen, $P_{f,N}$, can be calculated using the following equation.

$$P_{f,N} = P_{f,Al} + E_{fiber} \cdot \varepsilon_f \frac{t_{fiber}}{r_{FRP}} \cdot N. \tag{3}$$

In Fig. 7, the average of burst pressure in undamaged two-ply (Type ND-2) and three-ply specimens (Type ND-3) are close to each ROM value using the fracture strain of 2.5%, ε_f, obtained from the tensile tests of rovings. On the other hand, in the notched two-ply specimen (Type N-2), the maximum and burst pressure are lower than the ROM ($\varepsilon_f = 2.5\%$) value of one-ply as well as the two-ply specimen. In notched three-ply specimens, the maximum and burst pressure also result in the same as two-ply specimens.

If the strength of the inner ply of N-ply specimens ($N = 2, 3$) were maintained until the outermost ply was torn away, the burst pressure would be equivalent to the ideal burst pressure of $(N - 1)$-ply specimens at 2.5% strain. However, the burst pressure could not maintain each ROM ($\varepsilon_f = 2.5\%$) value.

4. DISCUSSION

In order to investigate the effect of length of teflon sheet on the strength, the relationship between the length of inserted teflon sheet and the strength in the three-ply specimen is shown in Fig. 8. In the figure, the initial ligament ratio, R, is defined by

$$R = \frac{L_c - L_{teflon}}{L_c} \times 100[\%], \tag{4}$$

where L_c and L_{teflon} are length of circumference of FRP layer ($=2\pi r_{FRP}$) and teflon sheet, respectively. When the outermost ply hoop strain of gage No. 1 was

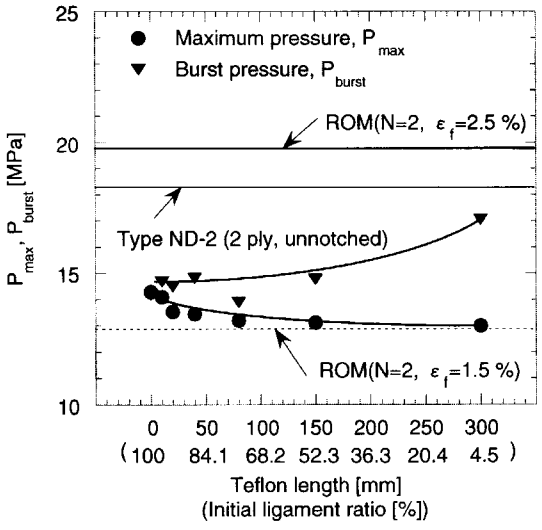

Figure 8. Relationship between teflon sheet length and strength in 3-ply specimen.

1.5% at the maximum pressure, P_{max}, half of the outermost ply was torn away (Fig. 4). Neglecting the contribution of the notched outermost ply to the strength, the maximum pressure can be estimated as the ROM value of two-ply assuming that the fracture strain, ε_f, is 1.5% instead of 2.5%. However, it can be seen in the figure that P_{max} is decreased and approaches the ROM value of two-ply ($\varepsilon_f = 1.5\%$) as the teflon sheet, i.e. pre-existing interlaminar delamination, becomes longer. Although further quantitative studies are needed, it is inferred that the contribution of the ligament to the maximum pressure is not negligible.

On the other hand, the burst pressure, P_{burst}, is increased as the pre-existing interlaminar delamination becomes longer. Especially, in the specimen with the longest teflon sheet, P_{burst} is close to that of the unnotched two-ply specimen as well as the ROM value of two-ply ($\varepsilon_f = 2.5\%$). If the inner ply was not damaged before all of the outermost ply was torn away, P_{burst} would maintain the burst pressure of the unnotched two-ply specimen. Consequently, it was suggested that the inner ply was damaged during the propagation of interlaminar delamination.

In order to investigate the effect of fracture path on P_{burst}, the specimens' appearance after the ring burst test were observed. Photographs of specimen appearance of shorter (Type N/T80-3) and longer teflon sheet (Type N/T300-3) after the ring burst test are shown in Fig. 9a and b, respectively. It can be seen in Fig. 9a that the fracture path deflects into the inner ply and the broken inner plies remain on the inside of the outermost ply. On the other hand, in Fig. 9b, it is observed that the fracture surface of the specimen with longer teflon sheet is flat and the delamination propagates smoothly. Therefore, it is suggested that in the specimen with shorter teflon sheet, the fracture path was deflected and the damage was expanded into the inner ply.

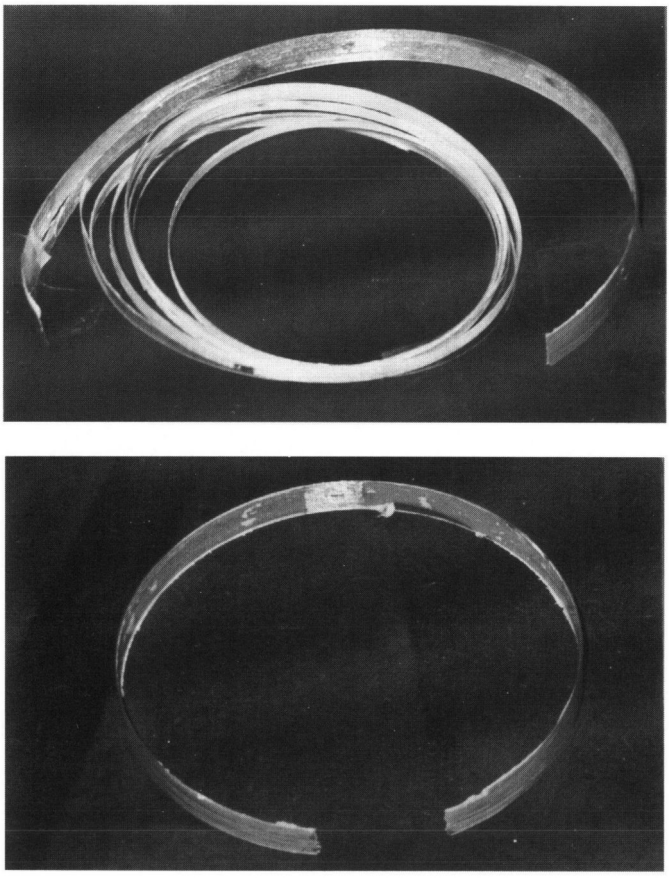

Figure 9. Photographs of fractured specimen appearance. (a) Specimen with shorter teflon sheet (Type N/T80-3). (b) Specimen with longer teflon sheet (Type N/T300-3).

Scanning electron micrographs of the inside surface of the outermost ply in the specimen with shorter and longer teflon sheet are shown in Fig. 10a and b, respectively. On the fracture surface of the shorter teflon sheet specimen, it is observed that the fiber roving is torn away from the outside of the inner ply and remained on the inside of the outermost ply. On the other hand, in the longer teflon sheet specimen, those fiber rovings on the fracture surface cannot be observed and the fracture surface is comparatively smooth.

It was deduced from Fig. 10 that in the longer pre-existing interlaminar delamination specimen, the interlaminar delamination propagated smoothly and the inner ply was not damaged. On the other hand, for the shorter pre-existing interlaminar delamination specimen, it was suggested that the expansion of damage into the inner ply was caused by the strong interlayer. Consequently, it can be proposed that in a specimen with the scratch in the outermost ply, the burst pressure can be strengthened by the control of interlaminar shear strength and the residual strength can be maintained by removing the damaged outermost ply appropriately.

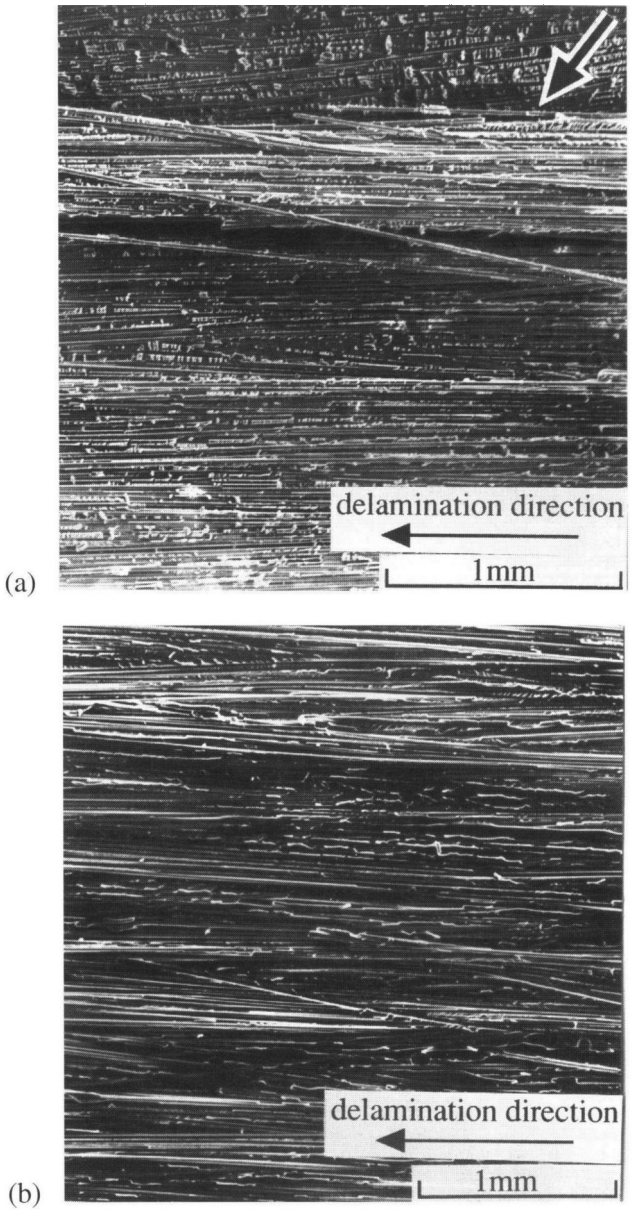

Figure 10. Scanning electron micrographs of the inside of outermost ply fracture surface. (a) Fiber roving torn away from the outside of inner ply (indicated by arrow). (b) Smooth fracture surface.

5. CONCLUSIONS

In this study, the propagation of delamination were characterized using an AE analysis, strain measurements and observations by an 8-mm camera and a high magnification video scope. Moreover, in order to evaluate the effect of fracture

path during test on the burst pressure, the macroscopic and microscopic fracture surface was observed.

From these results, the following conclusions were obtained:

(1) AE analysis is extremely useful for monitoring the propagation of delamination in FRP pressure vessel with damage.

(2) The maximum pressure is decreased as the pre-existing interlaminar delamination becomes longer due to the decreased contribution of the ligament.

(3) The burst pressure is decreased as the pre-existing interlaminar delamination becomes shorter because the fracture path is deflected and the damage is expanded into the inner ply.

REFERENCES

1. O. Fujishima, S. Wakayama and M. Kawahara, AE characterization of the fracture behavior during ring burst test of FW-FRP pressure vessel, in: *Progress in Acoustic Emission VII*, T. Kishi, Y. Mori, Y. Higo and M. Enoki (Eds), pp. 463–468. The Japan Society for Non-Destructive Inspection (1994).
2. A. Horide, S. Wakayama and M. Kawahara, in: *Proc. Japan Soc. Composite Materials 1998 Annual Meeting*, Tokyo, pp. 17–18 (1998).
3. H. Domae, Application of FRP composites cylinder to fire-man's breathing equipment, *J. High Press. Inst. Jpn.* **35**, 26–32 (1997).
4. T. Narushima, Current status of natural gas vehicles and FRP fuel container, *J. High Press. Inst. Jpn.* **35**, 9–14 (1997).
5. S. A. Matemilola and W. J. Stronge, Low-speed impact damage in filament-wound CFRP composite pressure vessels, *J. Pressure Vessel Tech.* **119**, 435–443 (1997).
6. H. Hyakutake and T. Yamamoto, Effects of notch geometry and fiber orientation on fracture characteristics of notched FRP plates under static load, *J. Soc. Mat. Sci., Japan* **44**, 401–406 (1995).
7. K. Kageyama, T. Kobayashi and K. Konaka, Mode I interlaminar fracture mechanics of unidirectionally reinforced carbon/epoxy laminates, *Trans. Jpn. Soc. Mech. Eng.* **53**, 1898–1904 (1987).
8. A. Todoroki and H. Kobayashi, Evaluation of delamination fracture toughness of high-strength CFRP and micromechanism, *Trans. Jpn. Soc. Mech. Eng.* **57**, 1648–1653 (1991).
9. K. Tohgo, A. S. D. Wang and T. W. Chou, A criterion for splitting crack initiation in unidirectional fiber-reinforced composites, *J. Compos. Mater.* **27**, 1054–1076 (1993).
10. A. Horide, S. Wakayama and M. Kawahara, Evaluation of strength in FW–FRP composites using ring burst test (effects of winding tension on fracture behavior and strength), *Trans. Jpn. Soc. Mech. Eng.* (in press).